

# Silver nanoparticle deposited implants to treat osteomyelitis

Samit Kumar Nandi,<sup>1</sup> Anish Shivaram,<sup>2</sup> Susmita Bose,<sup>2</sup> Amit Bandyopadhyay<sup>2</sup>

<sup>1</sup>Department of Veterinary Surgery and Radiology, West Bengal University of Animal and Fishery Sciences, Kolkata - 700037, India

<sup>2</sup>W. M. Keck Biomedical Materials Research Laboratory, School of Mechanical and Materials Engineering, Washington State University, Pullman, Washington 99164-2920, USA

Received 5 December 2016; revised 18 April 2017; accepted 22 April 2017

Published online 00 Month 2017 in Wiley Online Library (wileyonlinelibrary.com). DOI: 10.1002/jbm.b.33910

**Abstract:** In this study, electrolytically deposited strongly adherent silver nanoparticles on stainless-steel (SS) implants were used for *in situ* osteomyelitis treatment. Samples were heat treated to enhance adhesion of silver on 316 L SS. *Ex vivo* studies were performed to measure silver-release profiles from the 316 L SS screws inserted in equine cadaver bones. No change in the release profiles of silver ions were observed *in vitro* between the implanted screws and the control. *In vivo* studies were performed using osteomyelitic rabbit model with 3 mm diameter silver-deposited 316 L SS pins at two different doses of silver:

high and low. Infection control ability of the pins for treating osteomyelitis in a rabbit model was measured using bacteriologic, radiographic, histological, and scanning electron microscopic studies. Silver-coated pins, especially high dose, offered a promising result to treat infection in animal osteomyelitis model without any toxicity to major organs. © 2017 Wiley Periodicals, Inc. *J Biomed Mater Res Part B: Appl Biomater* 00B: 000–000, 2017.

**Key Words:** silver nanoparticle, osteomyelitis, stainless-steel implants, fracture management, infection control

---

**How to cite this article:** Nandi SK, Shivaram A, Bose S, Bandyopadhyay A. 2017. Silver nanoparticle deposited implants to treat osteomyelitis. *J Biomed Mater Res Part B* 2017;00B:000–000.

---

## INTRODUCTION

Osteomyelitis, an infective condition of the bone or bone marrow, is a severe and challenging setback in bone surgery. Various factors that can adversely influence osteomyelitis include poor surgical conditions that are typically seen in trauma cases, patient's habits such as smoking and drug addiction, and patients' health such as malnutrition and other immune deficiency disorders.<sup>1,2</sup> Furthermore, it has been observed that incidence of infection rate is between 5% and 10% of all inserted internal fixation devices; generally minor, between 0.5% and 2%, in closed fractures but as high as 30% for fixation of grade 3 open fractures.<sup>3</sup> Children mostly suffer from acute hematogenous osteomyelitis involving metaphysis of long,<sup>4</sup> whereas adults are the victim of subacute and chronic forms of osteomyelitis. Generally, osteomyelitis is commonly seen secondary to an open wound, most frequently an open injury to bone and surrounding soft tissues.<sup>5,6</sup> The incidence of deep musculoskeletal infection is reported to be as high as 23% from open fractures.<sup>7</sup> Patient-related factors that can further complicate this challenge include altered neutrophil defense, humoral immunity, and cell-mediated immunity. In a recent study, *Staphylococcus aureus* was concluded to be the most common organism isolated (43%) for osteomyelitis followed by *Pseudomonas aeruginosa* (10%), *Proteus* spp. (6%),

*Klebsiella* spp. (5%), *Escherichia coli* (5%), *Enterobacter* spp. (3%), *Staphylococcus epidermidis* (4%), *Streptococcus pyogenes* (2%), and *Enterococcus* spp. (2%).<sup>8</sup> Removal of the implant and dead tissue management are really the only satisfactory treatment options available at present in a clinical setting.

Antibiotics have been the go to remedy for such infections, but the use of antibiotics to prevent orthopedic surgical infections has been met with limited success over the years. Limited success has also been seen with nonantibiotic remedies such as chlorhexidine or nitrofurazone.<sup>9</sup> As an alternative therapy, use of silver as an antibiotic has come into wide use particularly in topical treatments. The use of silver has been seen for over thousands of years in many different civilizations. The effectiveness of silver relates to its broad spectrum of activity and its high chemotherapeutic ratio which is defined by the ratio of toxic dose to effective dose. Silver is biocidal in the ionic form.<sup>10,11</sup> Also, silver tends to show toxic effects toward microorganisms as compared to normal human cells and tissues.<sup>12–15</sup> Silver has also been used in FDA-approved devices, but mostly for short-term use in medical devices such as catheters. The key challenges to such an idea relates to maintaining effective silver concentration that is toxic to microorganisms but safe to normal healthy tissues, and long-term site-specific

**Correspondence to:** A. Bandyopadhyay; e-mail: amitband@wsu.edu

Contract grant sponsor: National Institute of Arthritis and Musculoskeletal and Skin Diseases of the National Institutes of Health; contract grant number: R01 AR067306-01A1

delivery. Over the years, use of silver directly or indirectly using various technologies has been researched upon showing the prevention of bacterial adhesion and emphasizing on its antimicrobial properties.<sup>16-18</sup> Previously, research has been performed in our group showing the effects of silver in various forms by directly depositing it on the surface as a strong adherent antimicrobial coating.<sup>1,13,19-21</sup> Recently, we have received our patent focusing on this technology from the United States Patent and Trademark Office.<sup>22</sup>

Owing to its good mechanical properties, corrosion resistance, and low cost, stainless steel is commonly used as standard implant material for fracture management. 316 L SS, where "L" stands for extra low carbon, composition in particular is widely used for fracture management devices as it does not bond with the bone which is an important factor taken into consideration.<sup>1</sup> Once a fracture is healed, many times the fracture management device such as a plate or nail needs to be taken out without damaging the fracture site.<sup>1</sup> However, for longer term implants that stay in the body such as hip and knee implants, typically titanium (Ti) and its alloys or CoCrMo are used in which good bone bonding ability is must to prevent implant loosening.

This work emphasizes on silver nanoparticle deposited 316 L SS implants for *in situ* treatment of osteomyelitis *in vivo*. Nanoparticulate silver coatings were applied to 316 L SS devices using an electrodeposition process. It should be taken into consideration that a wide range of experiments were performed during this process to find a suitable parameter for the silver deposition process. The adherence of silver to SS substrate was tested *ex vivo* by carrying out a silver release study with and without implantation into cadaver bone for a period of 7 days. The influence of silver coating for treating osteomyelitis in a rabbit model, shown in Figure 1, was evaluated by implanting samples into osteomyelitic rabbit femurs for a period of 42 days. Infection control ability of the silver-coated pins was measured using bacteriologic, radiographic, histological, and scanning electron microscopic studies. The main focus of this work demonstrates how strongly adherent nanoparticulate silver coatings can be added to an orthopedic device which when placed in an infected site can still prevent infection. Our emphasis is based on our recently patented work which focuses on this technology<sup>22</sup> and not to demonstrate the antimicrobial nature of silver which has been well established through many previous works.<sup>16-20</sup> In our case, in a rabbit model, within 42 days, such infection was cured, with high dose of silver showing good signs of curing infection as early as 21 days which is certainly not trivial.<sup>23-26</sup>

## MATERIALS AND METHODS

### Nanoparticulate silver deposition on 316 L SS

Commercially available medical grade 316 L SS screws of 2.7 mm in diameter and 16 mm in length were used for the *ex vivo* study. Samples were cleaned with DI water and ethanol prior to electrodeposition. An aqueous solution of 0.1 M AgNO<sub>3</sub> was used as an electrolyte for the process of electrodeposition and platinum foil was used as the anode material with the sample being the cathode. The electrodeposition

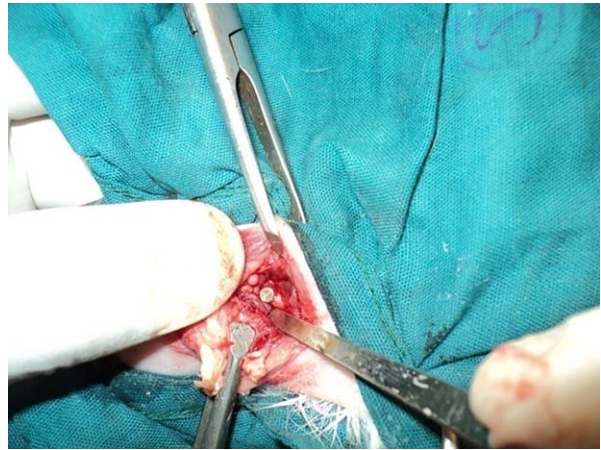


**FIGURE 1.** Photograph showing surgical implantation of silver coated 316L SS implants in distal femur of rabbit.

was performed using a DC power supply (Hewlett Packard 0-60 V/0-50 A, 1000 W) maintaining the voltage constant at 5 V for 40-45 s at room temperature, which resulted in a DC current in the range of 0.01-0.05 A. Postdeposition, the excessively loose silver particles resulting from the coating were gently wiped off from the surface using a tissue and DI water. Heat treatment at 500°C for 7 min under air atmosphere was performed using a vertical tube furnace and then the samples were cooled naturally at room temperature.<sup>1,21</sup> The process parameters were optimized after several experiments by varying the electrolyte concentration, electrodeposition time, and heat treatment conditions to achieve a nanoparticulate silver coating strongly adherent to the 316 L SS surface.<sup>1,13</sup> Silver dose can be controlled varying electrodeposition time. For 316 L SS pins for *in vivo* rabbit studies, 45 s (low dose) and 2 min (high dose) of electrodeposition times were used.

Characterization of the samples was performed using a field emission scanning electron microscope (FEI Quanta 200, FEI Inc., OR, USA) held at an operating voltage of 20 kV. SEM images of the silver-deposited samples were taken at regular intervals to optimize silver deposition parameters. Post-heat-treatment samples were cleaned with DI water before microscopic analysis. To confirm that the coating is in nanoparticle range, particle size analysis was performed using ImageJ software.

### *Ex vivo* silver release study in DI water

Nanoparticulate silver-deposited 316 L SS screws were placed in DI water for 7 days to study the release kinetics of silver upon implantation and cumulative silver release profiles were measured using an atomic absorption spectrophotometer (AAS, Shimadzu AA-6800, Shimadzu, Kyoto, Japan). Fresh DI water was replaced after each time point. Silver-deposited screws (performed under similar conditions) were studied under two different conditions only for low dose concentration: (1) screws implanted into an equine cadaver bone mimicking the surgical implantation procedure and (2) screws without the implantation, which

TABLE I. Design of Experiment for *In Vivo* Animal Experimentation

Groups	No of Animals	Implant	Days of Experiment	Experiment
Group I	3	No implants	3 weeks	Three animals were sacrificed for histological, radiographic, and microbiological examination to confirm development of osteomyelitis
Group II	6	Uncoated metal implants (control) in one femur and low-dose silver coating pin in another femur	After 3 weeks	Three animals were sacrificed for postoperative characterization
			After 6 weeks	Three animals were sacrificed for postoperative characterization
Group III	6	Uncoated metal implants (control) in one femur and high-dose silver coating pin in another femur	After 3 weeks	Three animals were sacrificed for postoperative characterization
			After 6 weeks	Three animals were sacrificed for postoperative characterization

was used as a control. Upon completion, the solution was analyzed for Ag<sup>+</sup> content using the AAS. The samples were tested in "Flame Mode" using air and acetylene (C<sub>2</sub>H<sub>2</sub>) fuel, and data collection was carried out using Shimadzu Wizaard software. The machine was calibrated using Ag<sup>+</sup> standards (High-Purity Standards, Charleston, SC, USA) of known concentrations from 0 to 5 µg/mL. During testing, a prespray time of 30 s and an integration time of 10 s were used. A release study of low and high dose of silver was also performed in phosphate-buffered saline (PBS) solution to identify the release profiles of both the doses. The release study was performed in a similar manner as mentioned above, and at each point, fresh solution was replaced.

#### ***In vivo* study in a rabbit model**

**Bacterial isolate.** *Staphylococcus aureus* was used for experimental model in rabbit. ATCC *S. aureus* culture (ATCC 29213) of 1 mL ( $5 \times 10^6$  CFU/mL) was injected into the medullary cavity of rabbit femur for successful induction of osteomyelitis and colony of the *S. aureus* was confirmed by growth in mannitol salt agar and other biochemical tests. Construction of successful osteomyelitic rabbit model using similar methods has been performed before and can be verified from our previous work.<sup>52,53</sup>

***In vivo* study.** All animal experimentations were performed in accordance to the standards of the Institutions Animal Ethical Committee of the West Bengal University of Animal and Fishery Sciences, India. Bone infection was induced in the femur (bilaterally) of 15 rabbits of 2–2.5 kg body weight under xylazine and ketamine hydrochloride anesthesia. Under strict aseptic measures, the medullary cavity of femurs was approached by a small incision followed by drilling using a 1.2 mm diameter drill and 1 mL of bacterial suspension (approximately  $3 \times 10^6$  CFU) of *S. aureus* was injected. The opening of drilled hole was closed using bone wax to prevent leakage of bacterial suspension into surrounding soft tissues. All the animals were observed for 3 weeks for development of osteomyelitis. Carprofen (4 mg/kg of body weight), a standard postoperative pain medication, was used for 3 days. The development of osteomyelitis

was confirmed by random radiography and selective histology and microbiological examination of swab from bone specimens of sacrificed rabbits (3 animals). After confirmation, a second surgery was done maintaining all standard formalities of surgery and silver-coated (both low and high dose) and uncoated stainless-steel implants were placed in the osteomyelitic bone, shown in Figure 1. All the samples were properly sterilized by autoclaving them at 121°C for 1 h. The detailed experimentation with these animals has been shown in Table I. The study samples were retrieved on days 21 and 42 postosteomyelitis development. Bone specimens containing the implants were decalcified in Goodling and Stewart's fluid-containing formic acid 15 mL, formalin 5 mL, and distilled water 80 mL solution. Histological examinations were carried out using hematoxylin and eosin-stained sections. Sequential radiographs (X-rays) from the infected bone were taken after osteomyelitis development and also from control and treated bone at 3 and 6 weeks. Implanted bones were also collected for SEM analysis from all the 3 groups (control, low-, and high-dose silver coating) after 21 and 42 days. The specimens were first fixed in E. M. grade 5% glutaraldehyde phosphate solution followed by washing twice for 30 min with PBS (pH 7.4) and distilled water. Dehydration of the samples was performed using a series of graded ethanol and finally with hexamethyldisilazane (HMDS) for final drying. Gold sputtered coating (JEOL ion sputter, Model JFC 1100, Japan) was performed on samples to make it conductive. The samples were then mounted into the resin and its surfaces were then examined under SEM (JEOL JSM 5200 model, Japan). After 21 days of postinduction of osteomyelitis, swab samples were also taken for microbiological examination for confirmation of osteomyelitis. Toxicological study of silver concentrations in major organs like heart, kidney, and liver was carried out at day 42 only.

## **RESULTS**

### **Characterization of nanoparticulate silver-deposited 316 L SS**

Figure 2(a,b) shows the scanning electron microscopy (SEM) images of deposited silver on the surface of 316 L SS

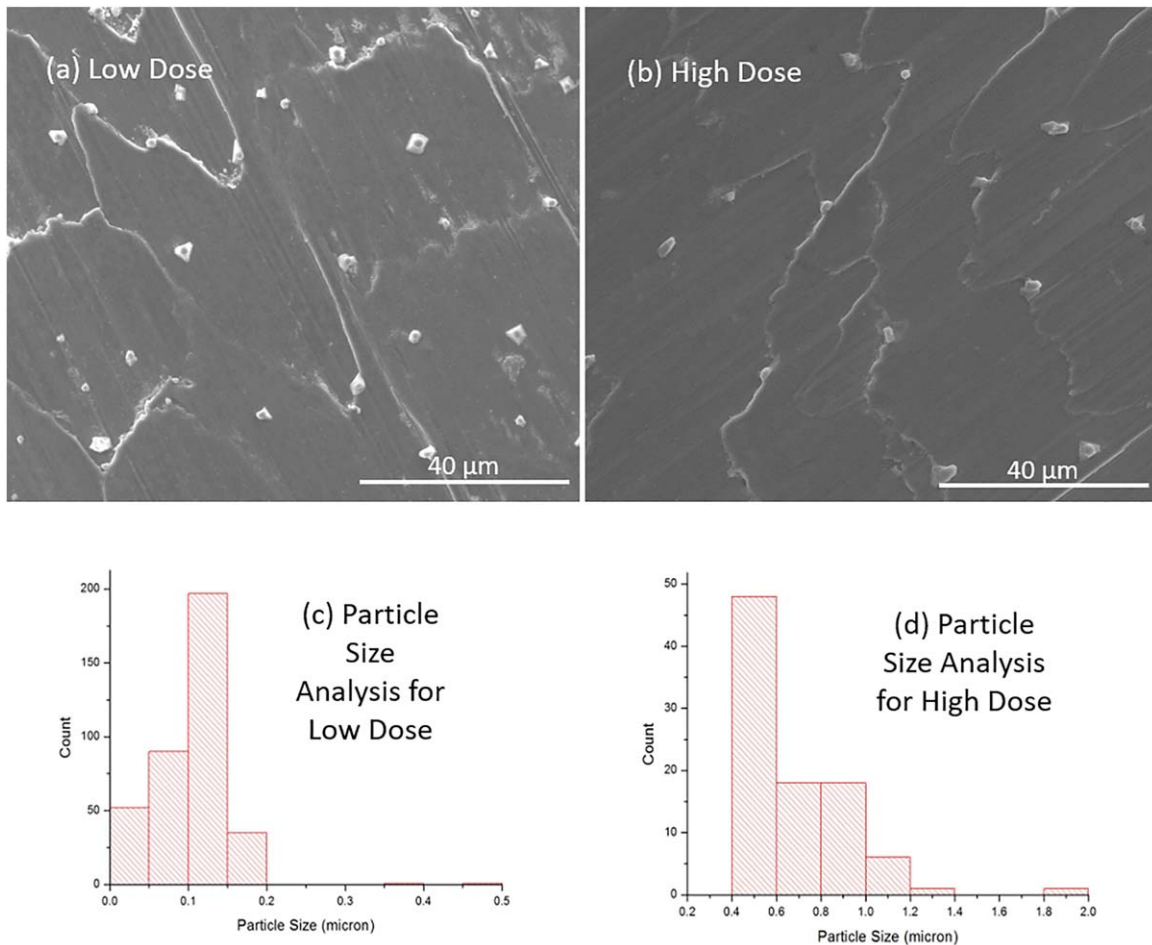


**FIGURE 2.** SEM images showing the deposition of silver particle on SS screw using (a) low dose of silver and (b) high dose of silver without any insertion into the bone. (c) Particle size analysis of low dose silver coating showing the coating is in nanoparticle range. (d) Particle size analysis of high dose silver coating showing the coating is in nanoparticle range.

screws using low and high dose of silver. The deposition resulted in a range of silver particles from nano- to micrometer sizes and proper measures were taken to remove the loosely adhered large particles on the surface by cleaning with DI water. Electrodeposition parameters were optimized to ensure that the deposition resulted with majority of the particles in the nanometer range. No significant differences can be seen in terms of silver particle size and distribution after the implantation due to strong adhesion of silver particles on 316 L SS surface. Such result is important to alleviate the concerns related to dislodging of silver particles due to friction and wear at the bone-SS screw interphase during surgical procedure. To confirm the nanoparticle coating of silver particle, size analysis of the coating was performed for low and high dose of silver as shown in Figure 2(c,d). Figure 3(a,b) shows the before and after implantation SEM images of silver-deposited 316 L SS screw surface.

#### Silver release study

Silver-deposited screws were implanted into the equine cadaver bone and the release of silver ions in DI water before and after implantation were studied for 7 days. Only

screws with low-dose concentration was considered for the *ex vivo* release study. Figure 3(c) shows the SEM image of the 316 L SS surface after 7 days of release study, clearly showing the presence of nanoscale silver particles on the surface. This images strong adhesion of particles to the surface and long-term silver release ability from the device. Figure 3(d) shows the release profiles of the silver ions when implanted into the cadaver bone *ex vivo*, and without implantation, that is, as control. No significant changes in the release profiles can be seen due to *ex vivo* implantation. Also, an initial fast release rate in the first 3 days can be observed after which silver release rate gradually decreases in both cases. The total cumulative release observed for silver ions in both cases are within the potential toxic limit of 10 ppm ( $\mu\text{g}/\text{mL}$ ) mentioned for the human cells,<sup>1</sup> a key factor dealing with silver technologies. Similar 7-day release study was performed for low- and high-dose coated silver in phosphate-buffered saline (PBS) solution to get an idea of both the doses of release profiles in buffered saline environment. The cumulative release of silver ions in both doses was within the toxic limit mentioned for human cells, that is, 10 ppm ( $\mu\text{g}/\text{mL}$ ) as shown in Figure 3(e).<sup>1</sup>

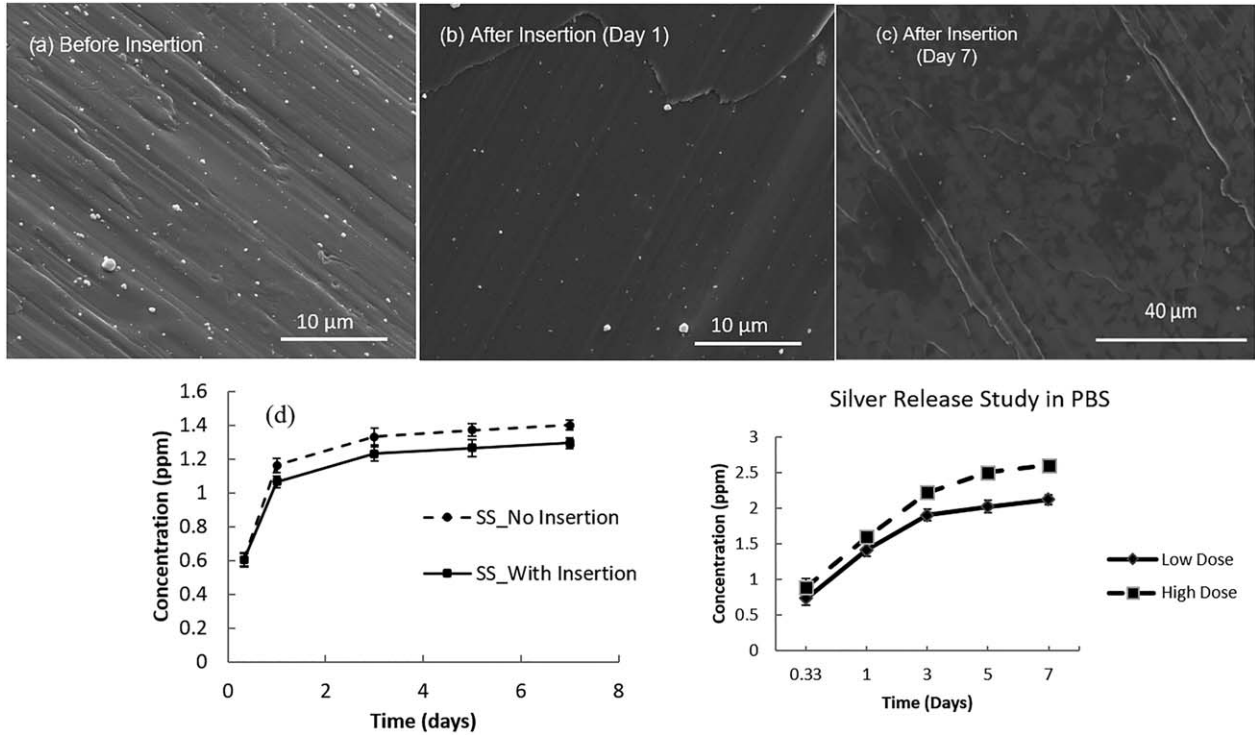


**FIGURE 3.** SEM images showing the electrodeposition of silver particles (a) before insertion to equine cadaver bone, (b) after insertion, and (c) after 7 days in media. Presence of silver particles on the surface can be seen in all the cases. (d) Cumulative release profiles from silver-electrodeposited 316 L SS screws for 7 days with insertion and without insertion into the equine cadaver bone performed in DI water. (e) Cumulative silver release profiles of stainless-steel screws with low- and high-dose silver deposition for 7 days without insertion in PBS (phosphate-buffered saline).

**Microbiological examination**

The swab specimens collected from the bone specimens of group I animals after 21 days were streaked on mannitol 10% salt agar slant and incubated at 37°C for overnight. Observations showed characteristic bacterial growth, sample was collected from a single colony bacterial growth which was stained by Gram’s staining method. The organisms

were gram (+) coccoid and arranged in single or diploid similar to the organism inoculated (Figure 4). The swab specimens were also collected from the implanted site of bone in all the groups at days 21 and 42 and inoculated in mannitol 10% salt agar and incubated at 37°C for overnight. No bacterial growth of *S. aureus* was found except in control group where such growth was seen.

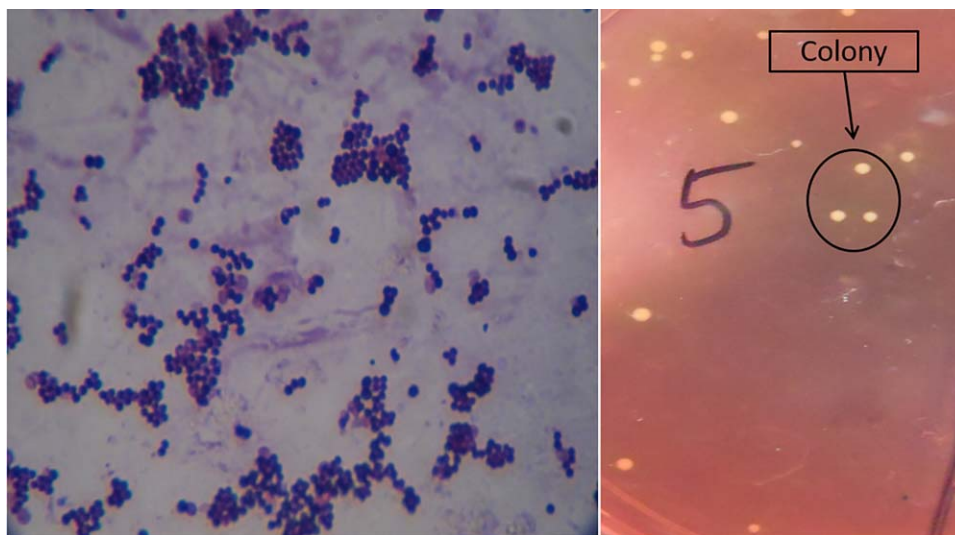


**FIGURE 4.** Photograph showing characteristic morphology of *Staphylococcus* (left) and characteristic colony of *Staphylococcus* in mannitol agar 10% slant after overnight incubation (right).

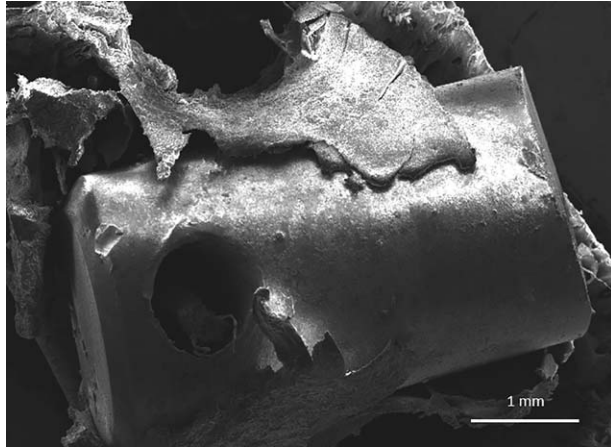


**FIGURE 5.** SEM microstructure of bone defect site for control groups of animals taken after 42 days.

### Scanning electron microscopy of cortical bone

Microstructures of bone defect sites for all the groups of animals are shown in Figures 5–7. Control pin implanted bone sample shows no appreciable bone formation due to presence of infection. There is decalcification of the bony matrix with osteolytic activity and insignificant presence of bridging callus and fibro cartilaginous tissues in Figure 5. Low-dose silver-deposited sample after 21 days shows initiation of bone apposition around the surface of pin as observed by newly formed collagen fibrils. Whereas in 42 days, collagen fibril formation vis-à-vis new bone formation is more compared to earlier day, that is, day 21 and is shown in Figure 6. High-dose silver-deposited pins implanted bone after 21 days shows more bone formation around the pin surface as observed by better communication of collagen fibrils although some interfacial gap is there. At 42 days, there is presence of abundant collagenous tissue around the pin surface along with formation of matured bone and shown in Figure 7.

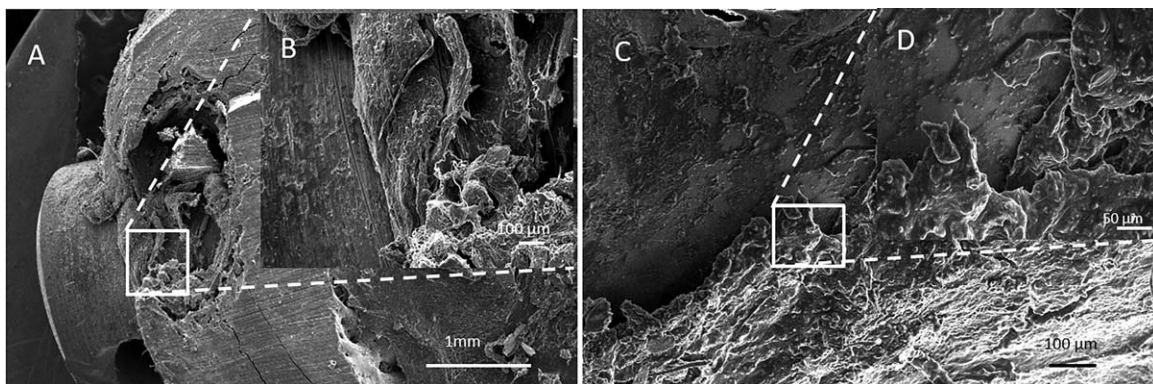
### Radiological examinations

Figure 8 shows the radiographs of all three groups at different times. Typical radiographic evidences of osteomyelitis in animals of all groups are presence of severe periosteal

reaction in the distal femur with lytic changes and thinning. In some places of distal femur, spongy bone appearance was not clearly visible. Radiodensity of bone marrow appeared to be in excess with mild endosteal reaction in Figure 8(A1). Radiographically, control sample at days 21 and 42 shows increased radiodensity along with the loss of characteristics of cancellous bone in distal femur and presence of both the phytic and lytic changes. Endosteal reaction was moderate and clearly visible. Interruption of cortical border of distal femur is evident in some places along with secondary osteophytic changes of epiphyseal cartilage, as shown in Figure 8(C21 and C42). The radiograph on 21 days in low-dose silver-coated bone sample shows discontinuation of cortex in few places with mild endosteal reaction. Presence of mild radiolucent zones in metaphyseal region of femur is characteristic of osteoclastic changes. At day 42, the radiograph shows absence of periosteal reaction and discontinuation of cortex as observed in earlier days. Restoration of the medullary cavity and remodeling of cortex is prominent although there is presence of few radiolucent zones in epiphysis, as shown in Figure 8(L21 and L42). In high-dose silver-deposited pins on day 21 and 42 show lack of periosteal and endosteal reaction, clear medullary cavity along with cortical continuation as observed from the radiographs, shown in Figure 8(H21 and H42).

### Histological examination

Figure 9 shows the histological evaluation at the bone-implant interface for all groups. Histological section of femur bone in group I revealed bony degeneration of haversian plates with infiltration of mononuclear cells and few osteoblasts in medullary sinuses. There is evidence of osteoclastic activity in some interstitial spaces and the margin of sinuses is getting worn out in some places. The total phenomena were indicative of osteomyelitis and shown in Figure 9(A1). In control group with no silver coating, osteomyelitic changes are seen on days 21 and 42 characterized by degenerative changes of hemopoiesis center, osteophytes, fat cells along with mild fibrovascular proliferation of connective tissues. Bone marrow in the peripheral region showed penetration with mononuclear cells and osteoclasts penetration was observed in the bone marrow



**FIGURE 6.** SEM microstructures of bone defect sites for low-dose silver-coated implants of animals taken after (A,B) 21 days and (C,D) 42 days.

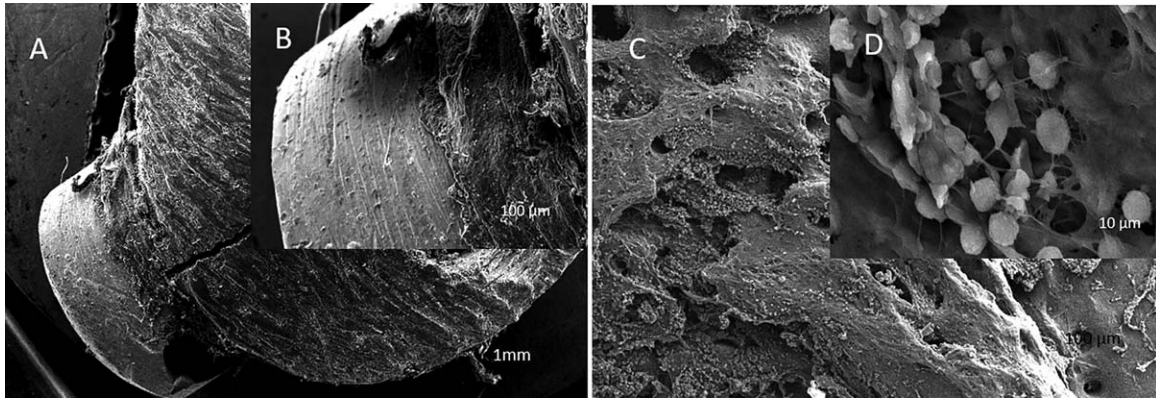


**FIGURE 7.** SEM microstructures of bone defect sites for high-dose silver-coated implants of animals taken after (A,B) 21 days and (C,D) 42 days.

peripheral region which is shown in Figure 9(C21 and C42). As shown in Figure 9(L21), with low-dose silver-coated samples on day 21, presence of Haversian canal along with sinusoidal spaces filled with red blood cells (RBC), mononuclear cells, and mucin threads. Infiltration of osteoblast along with mononuclear cells is seen at some places. Fibrovascular reaction is seen all throughout the parenchymatous

region. On day 42, as shown in Figure 9(L42), section depicted a well-developed vascular stroma of bony plates characterized by newly formed Haversian canals tightly all throughout the structure. Osteoblastic and osteoclastic activities are moderate to severe. Fibrosis in subcortical area is also evident indicating a good response to healing. Histological sections of high-dose silver coating on day 21 [Figure

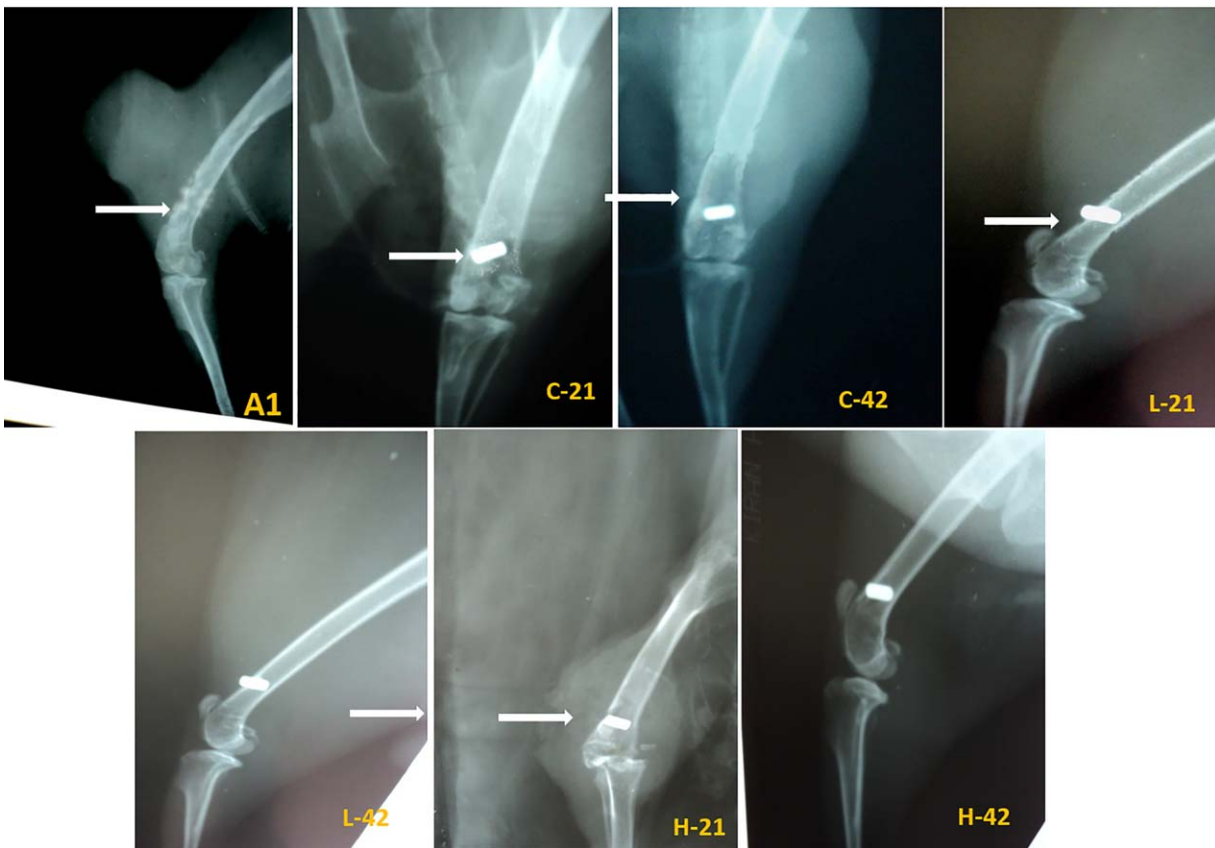


**FIGURE 8.** Radiographic pictures of distal femur showing the following: A1, Development of osteomyelitis after 21 days. The osteophytic and lytic changes are shown in osteomyelitis. C21 and C42, Control sample at 21 and 42 days showing osteophytic and lytic changes along with discontinuation of cortical border of distal femur. L21 and L42, Low-dose silver-coated sample showing discontinuation of cortex in few places with mild endosteal reaction at day 21 and absence of periosteal reaction and discontinuation of cortex at day 42. H21 and H42, High-dose silver-coated sample at 21 and 42 days showing recovery from the osteomyelitis changes at the adjacent area of implant.

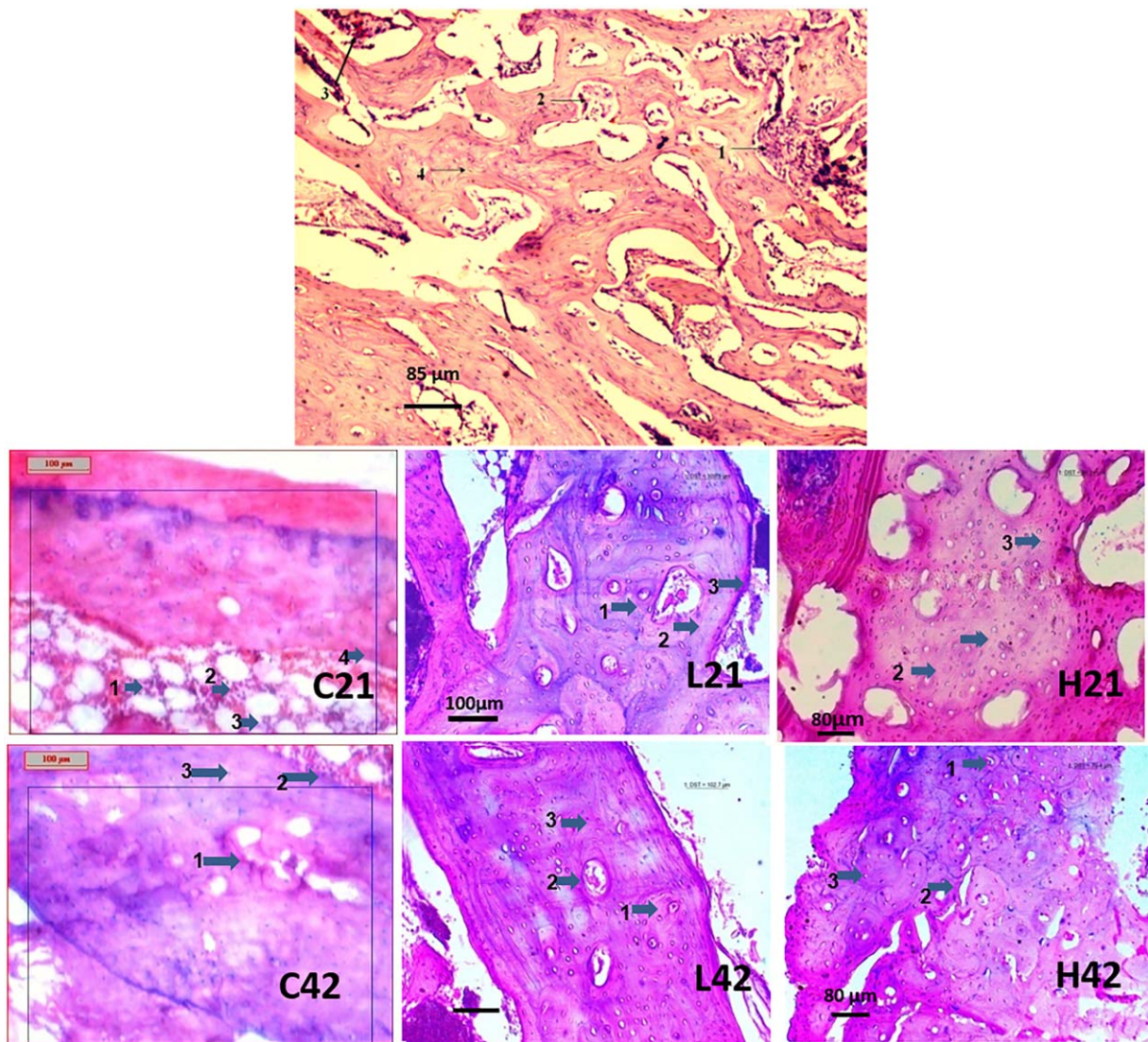


**FIGURE 9.** A1, Histological section of development of osteomyelitis after 21 days (1, clusters of osteoblast and osteoclast; 2, RBCs and mononuclear cells; 3, medullary cavity; 4, intraosseous septa). C21 and C42, Histology of control sample after 21 and 42 days after development of osteomyelitis (C21: 1, clumping of RBCs and mononuclear cells; 2, mononuclear cell and osteoclast; 3, fat cells; 4, blood vessels and fibroblast. C42: 1, fibroblastic proliferation; 2, aggregation of mononuclear cell and osteoclast; 3, degenerative changes in bony lamellae). L21 and L42: Histology of bone section of Ag-coated low-dose implant at 21 and 42 days (L21 and L42: 1, Haversian canal; 2, fibrovascular proliferation; 3, mononuclear cell and osteoblast). H21 and H42: Histology of bone section of Ag-coated high-dose implant at 21 and 42 days (H21: 1, Haversian canal; 2, fibrovascular lamellae; 3, mononuclear cell and osteoblast. H42: 1, Haversian canal; 2, sinusoidal space; 3, fibrovascular proliferation).

9(H21)] shows well-defined Haversian system along with canalicular structure and formation of osteoclastic foci with infiltration of mononuclear cells. There was mucinous degeneration at the central level of Haversian canal. Vascularization at few points was suggestive of angiogenesis which indicated a tendency to repair the parenchymatous mass. Some of the inner lining of canaliculi reveal acellular cystic lining along with void mass in their lumina. Collagen fibers and immature fibroblast run in few places. There is tendency to extravasations of RBC in pericortical zone of Figure 9(H21). On day 42, section shows a multiple number of Haversian canals tightened by a delicate bundle of fibrous tissue. Vascular proliferation is prominent particularly to the periphery of canal and inner side of medullary region.

Mucin secretion is seen in few places. Proliferation of mononuclear cells is low although the structure is tightly embedded by osteoblast and osteoclast cells. Thickening of vessel wall due to good proliferation of osteoblast cell causes partial compression of sinusoidal places, and shown in Figure 9(H42).

#### Toxicological examination

Toxicological study of silver concentrations in major organs such as heart, kidney, and liver was carried out at day 42 only. Based on high-performance liquid chromatography (HPLC) estimation of silver concentration on day 42, it has been measured that the concentration of silver in high-dose pin in Heart-BDL (below detection limit), Kidney-0.53 ppb,



liver-1.02 ppb and in low-dose pin Heart-BDL (below detection limit), Kidney-0.41 ppb, liver-0.38 ppb. All concentrations were below the toxicity levels advised for silver. At the time of sacrifice, the animals were healthy and fit without any undesirable side effects.

## DISCUSSIONS

Owing to the lack of treatment options, osteomyelitis patients become disappointed to the therapeutic outcomes. Typically, early antibiotic therapy is the ideal option that must be administered for at least 4–6 weeks or more to achieve an acceptable rate of cure.<sup>5,27</sup> However, if antibiotic therapy fails, adequate debridement, drainage of pus, and prolonged courses of parenteral antibiotics for another 4- to 6-week course is needed.<sup>27,28</sup> The treatment of chronic osteomyelitis is more complex and generally requires approaches such as combination of infection control and radical debridement,<sup>29</sup> fracture stabilization in case of non-union or bone segment excision, antimicrobial therapy, dead space and wound management, and provision of bone graft substitutes, especially in the case of large bone defects.<sup>30,31</sup> Conventional antimicrobial therapy fails to provide satisfactory results in many cases due to physiological differences in blood supply, local vascularization, and the presence of “blood–bone” barrier.<sup>32</sup> The limitations of systemic antibiotic therapy include prolonged treatment due to being unable to create a high local concentration and the consequential risk of toxicity.<sup>33–36</sup> Moreover, impaired vascularity of osteomyelitis bone requires the use of higher doses of antibiotics due to poor antibiotic penetration and the difficulty in eradicating organisms when they are in a biofilm phase.<sup>36</sup> In spite of standard care, therapeutic failures and reappearances are common, sometimes as high as 30%.<sup>36–40</sup>

Control of infection on and around SS implants is usually difficult and may lead to ultimate implant migration.<sup>41,42</sup> Preventive measures are sought by the researchers to overcome implant-related infection vis-à-vis to give relief to the ailing patient. Various approaches have been attempted to make SS implant surface antibacterial either by impregnation of the surface with antibiotics<sup>43</sup> or coating of the surface with silver that may cause sustained release of drugs during application.<sup>44–47</sup> We hypothesized that strongly adherent silver nanoparticles on the stainless-steel implant will have *in situ* antibacterial properties as a treatment option for osteomyelitis for an extended period of time *in vivo*. The antibacterial activity of silver is well established<sup>45,46</sup> and mostly relies on the silver cation  $\text{Ag}^+$ , which has a property to bind to electron donor groups of sulphur, oxygen, or nitrogen in biological molecules. Generally, oxidation of metallic silver to the active state ( $\text{Ag}^+$ ) occurs via an interaction of the silver in aqueous setting.<sup>48</sup> Silver has broad spectrum antibacterial properties against both Gram-positive and Gram-negative bacteria and even in some drug-resistant bacteria at very low concentrations (ppb level).<sup>49</sup> Silver coatings have been made in many clinical contexts such as heart valves, central venous catheters, and urinary catheters and have proved to minimize infection rate toward

short-term use of medical devices.<sup>50,51</sup> However, to the best of our knowledge, scanty in-depth published data available on silver-deposited stainless-steel implants for the *in situ* treatment of osteomyelitis.

We developed low and high concentration of silver deposited 316 L SS implants and compared with control sample without silver. The minimum requirement of an implant to be bactericidal is steady and continuous release of silver ions at concentration levels of at least 0.1 ppb.<sup>52</sup> For *ex vivo* characterization, only low dose/concentration was used as both the doses resulted in coatings with similar particle range. The silver deposition was carried out using electrodeposition process which is a cost effective method. The electrodeposition resulted in a coating ranging from micro- to nanoparticles. Efforts were taken to ensure the resulting coating contains mostly nanoparticle by cleaning them with DI water. But electrodeposition of silver nanoparticles on SS surface can led to poor adhesion, and required further heat treatment which was performed at 500°C. The cumulative release of silver ions is found to be well below the toxic limit specified for the human tissue. World Health Organization (WHO) recommends no observable adverse effect level (NOAEL) of silver up to 10 g for a normal human being.<sup>53</sup> The most serious concern for silver toxicity is Argyria, which is not found at or below 1.7 g total silver *in vivo*. Researchers have reported that silver intake from the diet can be between 27 and 88  $\mu\text{g}/\text{day}$ .<sup>11</sup>

To test the antibacterial properties of silver-deposited 316 L SS, *S. aureus*, the commonly involved bacteria in development of osteomyelitis was chosen.<sup>54,55</sup> Amid the animal trial results, histopathological and microbiological findings are the most important tools for detection of the efficiency of treatment of osteomyelitis and implant–host bone reaction.<sup>56</sup> Based on the histological analysis, the tendency of alleviating infection and intramedullary new bone formation was higher in high-dose silver-deposited implants followed by low-dose implant when compared to control samples. In low-dose samples, mild infective changes were noticed on day 21 but subsided gradually with the passage of time on day 42. Whereas high-dose sample showed complete eradication of infection on days 21 and 42 with development of multiple number of Haversian canals, vascular proliferation and tightly embedding by osteoblast and osteoclast cells with no periosteal reaction in and around the osteomyelitis area. These findings confirm a better efficacy of these implants to resist the injected *S. aureus*. The silver ions may be released in sufficient concentration from the implants, which combines to membranes, enzymes, and nucleic acids leading to a variety of reversible and irreversible cellular intervention.<sup>46,57</sup> Moreover, presence of silver ions may hinder the respiratory chain vis-a-vis the aerobic metabolism of causative microorganisms.<sup>58</sup> High-dose silver has the capacity to inhibit bacterial adhesion and growth without altering the activity of osteoblasts and epithelial cells.<sup>59</sup> In low-dose samples, the efficacy of silver ions in treating osteomyelitis on day 21 was less due to low silver concentrations available in the area. This may be due to interference of mode of action of silver ions with the murein

of the bacterial cell wall as reported earlier.<sup>60</sup> Microbiological examinations were also carried out in each time point. The minimum concentration of 10–40 ppb of silver ion is necessary to kill the most pathogenic microorganisms and 60 ppb to eliminate the most resistant strains including methicillin-resistant *S. aureus*.<sup>61</sup> In this study, it is expected that this minimum concentration was available at the surface of the implants.

Radiological findings of osteomyelitis show the presence of severe periosteal reaction with lytic changes, absence of spongy bone appearance with more radiodensity of bone marrow.<sup>62</sup> With the passage of time, these findings are completely absent in high-dose silver samples on both days 21 and 42; however, in low-dose sample, initially, there was presence of osteomyelitis signs of mild endosteal reaction along with presence of mild radiolucent zones which subsided gradually on day 42. It has been reported that silver-coated prostheses show lower infection rates against *S. aureus*, without any undesirable side effects on the surrounding tissues.<sup>47</sup> Silver-coated polymer and stainless-steel pins also confirmed similar results without any cytotoxicity.<sup>46</sup> Microstructure of bone–biomaterial interfaces of uncoated implants show no appreciable bone formation due to presence of infection. Low-dose samples show less bone apposition around the surface in earlier days that increases gradually with the passage of time. This may be due to presence of residual infection in earlier days. High-dose sample shows bone formation around the implant surface as observed by better communication of collagen fibrils both on days 21 and 42, which shows the potentiality of silver ions in eradicating the infection in osteomyelitis site.

Finally, silver concentrations in the vital organs such as heart, kidney, and liver were within the normal range in both low- and high-dose silver-coated implants. Silver levels below 10 ppb were regarded as normal.<sup>63</sup> Toxicological side effects are noticed for silver when blood concentration is >300 ppb in the form of argyrosis, leukopenia, liver, and kidney damage.<sup>64</sup> However, in this study, silver concentrations were well below the critical concentration, and no such toxicological side effects were observed.

## CONCLUSIONS

316 L SS implants were coated with silver nanoparticles via electrodeposition for 45 s (low dose) and 2 min (high dose) in 0.1 M silver nitrate solution as an electrolyte. Postdeposition heat treatment was done at 500°C for 7 min to increase adhesion of silver nanoparticles on the 316 L SS surface per our patented technology. *Ex vivo* implantation on equine cadaver bone followed by silver release study in DI water and microscopic analysis confirm that no measurable degradation on the surface to dislodge the silver particles during surgical procedure.

Direct ability to treat osteomyelitis using strongly adherent nanoparticulate high- and low-dose silver-deposited nails was studied using a rabbit model followed by bacteriologic, radiographic, histological, and scanning electron microscopic study. Silver-deposited pins, especially high

dose, offered a promising result in terms of eradication of infection in rabbit osteomyelitis model without any toxicity in major organs such as heart, kidney, and liver on both 21 and 42 day points. Based on our findings, we can conclude that strongly adherent nanoparticles silver on 316 L SS surface can effectively treat osteomyelitis. Such findings are especially important because apart from the removal of implant or dead tissue management, there are no satisfactory treatment options available at present for osteomyelitis in a clinical setting.

## ACKNOWLEDGMENTS

SN would like to thank Vice Chancellor of West Bengal University of Animal and Fishery Sciences for support during the animal research work. The content is solely the responsibility of the authors and does not necessarily represent the official views of the National Institutes of Health.

## REFERENCES

1. Devasconcellos P, Bose S, Beyenal H, Bandyopadhyay A, Zirkle LG. *Mater Sci Eng C* 2012;32:1112–1120.
2. Malizos KN, Gougoulas NE, Dailiana ZH, Varitimidis S, Bargiotas KA, Paridis D. *Injury* 2010;41:285–293.
3. Megas P, Saridis A, Kouzelis A, Kallivokas A, Mylonas S, Tyllianakis M. *Injury* 2010;41:294–299.
4. Carek PJ, Dickerson LM, Sack JL. *Am Fam Physician* 2001;63:2413–2421.
5. Haas DW, McAndrew MP. *Am J Med* 1996;101:550–561.
6. Lew DP, Waldvogel FA. *N Engl J Med* 1997;336:999–1007.
7. Gustilo RB. Management of infected fractures. In: Evarts CM, et al., editors. *Surgery of the Musculoskeletal System*, Vol. 5, 2nd ed. New York: Churchill Livingstone; 1990; pp 4429–4453.
8. Kaur J, Gulati VL, Aggarwal A, Gupta V. *Indian J Practising Doctor* 2008;4.
9. Prince HN, Prince DL. *Orthoped Des Technol* 2008.
10. Tripton IH, Cook JM. *Health Phys* 1963;9:103–145.
11. Hamilton EI, Minski MJ, Cleary JJ. *Sci Total Environ* 1972;1:341–374.
12. Schierholz J, Lucas L, Rump A, Pulverer G. *J Hosp Infect* 1998;40:257–262.
13. Das K, Bose S, Bandyopadhyay A, Karandikar B, Gibbins BL. *J Biomed Mater Res B* 2008;87:455–460.
14. Kokubo T, Kushitani H, Sakka S, Kitsugi T, Yamamuro T. *J Biomed Mater Res* 1990;24:721–734.
15. Ohtsuki C, Kokubo T, Neo M, Kotani S, Yamamuro T, Nakamura T, Bando Y. *Phosphorus Res Bull* 1991;1:191–196.
16. Matthew ED, Luckarift HR, Johnson GR. *ACS Appl Mater Interfaces* 2009;1:1553–1560.
17. Pollini M, Paladini F, Catalano M, Taurino A, Licciulli A, Maffezzoli A, Sannino A. *J Mater Sci Mater Med* 2011;22:2005–2012.
18. Gao A, Hang R, Huang X, Zhao L, Zhang X, Wang L, Tang B, Ma S, Chu PK. *Biomaterials* 2014;35:4223–4235.
19. Roy M, Fielding GA, Beyenal H, Bandyopadhyay A, Bose S. *ACS Appl Mater Interfaces* 2012;4:1341–1349.
20. Fielding GA, Roy M, Bandyopadhyay A, Bose S. *Acta Biomater* 2012;8:3144–3152.
21. Shivaram A, Bose S, Bandyopadhyay A. *J Mech Behav Biomed Mater* 2016;59:508–518.
22. Bandyopadhyay A, Bose S. Materials with modified surface and methods of manufacturing, US Patent 9,440,002.
23. Brennan SA, Ní Fhoghlú C, Devitt BM, O'Mahony FJ, Brabazon D, Walsh A. *Bone Joint J* 2015;97:582–589.
24. Kose N, Çaylak R, Pekşen C, Kiremitçi A, Burukoglu D, Koparal S, Doğan A. *Injury* 2016;47:320–324.
25. Qin H, Cao H, Zhao Y, Zhu C, Cheng T, Wang Q, Peng X, Cheng M, Wang J, Jin G, Jiang Y, Zhang X, Liu X, Chu PK. *Biomaterials* 2014;35:9114–9125.
26. Harrasser N, Gorkotte J, Obermeier A, Feihl S, Straub M, Slotta-Huspenina J, Eisenhart-Rothe R, Moser W, von Gruner P, deWilde

- M, Gollwitzer H, Burgkart R. *BMC Musculoskeletal Disord* 2016;17:1.
27. Mader JT, Shirliff ME, Bergquist SC, Calhoun J. *Clin Orthop* 1999;360:46–65.
  28. Mader JT, Mohan D, Calhoun J. *Drugs* 1997;54:253–64.
  29. Tetsworth K, Cierny G. *Clin Orthop Relat Res* 1999;360:87–96.
  30. Nandi SK, Mukherjee P, Roy S, Kundu B, De DK, Basu D. *Mater Sci Eng C Mater Biol Appl* 2009;29:2478–2485.
  31. Lazzarini L, Mader TT, Calhoun JH. *J Bone Joint Surg Am* 2004;86:2305–2318.
  32. Walenkamp GH, Vree TB, van Rens TJ. *Clin Orthop Relat Res* 1986;205:171–183.
  33. Narahariseti PK, Lew MDN, Fu YC, Lee DJ, Wang CH. *J Control Release* 2005;102:345–359.
  34. Billon A, Chabaud L, Gouyette A, Bouler JM, Merle C. *J Microencapsul* 2005;22:841–852.
  35. Xu QG, Czemuszka JI. *J Control Release* 2008;127:146–153.
  36. El-Husseini M, Patel S, MacFarlane RJ, Haddad FS. *J Bone Joint Surg Am* 2011;93:151–157.
  37. Schnieders J, Gbureck U, Thull R, Kissel T. *Biomaterials* 2006;27:4239–4249.
  38. Kanellakopoulou K, Thivaos GC, Kolia M, Dontas I, Nakopoulou L, Dounis E, Giamarellos-Bourboulis EJ, Andreopoulos A, Karagiannakos P, Giamarellou H. *Antimicrob Agents Chemother* 2008;52:2335–2339.
  39. Lipsky BA, Berendt AR, Deery HG, Embil JM, Joseph WS, Karchmer AW, Lefrock JL, Lew DP, Mader JT, Norden C, Tan JS. *Diagn Treat Diabet Foot Infect* 2004;39:885–910.
  40. Tice AD, Hoaglund PA, Shoultz DA. *Am J Med* 2003;114:723–728.
  41. Respet PJ, Kleinman PG, Meinhard BP. *J Orthop Res* 1987;5:600–603.
  42. Bhattacharyya M, Bradley H. *Wounds* 2006;2:26–34.
  43. Parvizi J, Wickstrom E, Zeiger AR, Adams CS, Shapiro IM, Purtill JJ, Sharkey PF, Hozack WJ, Rothman RH, Hickok NJ. *Clin Orthop Relat Res* 2004;429:33–38.
  44. Böswald M, Lugauer S, Regenfus A, Greil J, Guggenbichler JP. *Infection* 1999;27:24–29.
  45. Olson ME, Harmon BG, Kollef MH. *CHEST J* 2002;121:863–870.
  46. Brutel de la Riviere A, Dossche KM, Birnbaum DE, Hacker R. *J Heart Valve Dis* 2000;9:123–9.
  47. Bosetti M, Massè A, Tobin E, Cannas M. *Biomaterials* 2002;23:887–892.
  48. Melaiye AYW. *Expert Opin Therap Pat* 2005;15:125–130.
  49. Cook G, Costerton JW, Darouiche RO. *Int J Antimicrob Agents* 2000;13:169–173.
  50. Davenport K, Keeley FX. *J Hosp Infect* 2005;60:298–303.
  51. Kumar R, Munstedt H. *Biomaterials* 2005;26:2081–2088.
  52. Kundu B, Nandi SK, Roy S, Dandapat N, Soundrapandian C, Datta S, Mukherjee P, Mandal TK, Dasgupta S, Basu D. *Ceram Int* 2012;38:1533–1548.
  53. Kundu B, Soundrapandian C, Nandi SK, Mukherjee P, Dandapat N, Roy S, Datta BK, Mandal TK, Basu D, Bhattacharya RN. *Pharm Res* 2010;27:1659–1676.
  54. Joosten U, Joist A, Frebel T, Brandt B, Diederichs S, von Eiff C. *Biomaterials* 2004;25:4287–4295.
  55. Hollinger MA. *Crit Rev Toxicol* 1996;26:255–260.
  56. Bragg PD, Rainnie DJ. *Can J Microbiol* 1974;20:883–889.
  57. Chen W, Liu Y, Courtney HS, Bettenga M, Agrawal CM, Bumgardner JD, Ong JL. *Biomaterials* 2006;27:5512–5517.
  58. Modak K, Fox C. *Biochem Pharm* 1973;22:2392–2404.
  59. Burrell RE. Silver release in simulated wound fluids from silver containing dressings. 2nd Meeting of World Wound Healing Societies, Paris: Abs. Z.042; 2004.
  60. Nandi SK, Kundu B, Mandal TK, De DK, Basu D. *Ceram Int* 2009;35:1367–1376.
  61. Gosheger G, Harges J, Ahrens H, Streitburger A, Buerger H, Erren M, Gonsel A, Kemper FH, Winkelmann W, von Eiff C. *Biomaterials* 2004;25:5547–5556.
  62. Greil J, Spies T, Böswald M, Lugauer S, Regenfus A, Guggenbichler JP. *Infection* 1999;27:34–37.
  63. Chambers C, Proctor C, Kabler P. *J Am Water Works Assoc* 1962;54:208–216.
  64. World Health Organisation. Silver in Drinking Water: Background Document for the Development of WHO Guidelines for Drinking Water Quality. Geneva, Switzerland: WHO; 1996. WHO/SDE/WSH/03.04/14.